Journal of Mechanical Science and Technology 29 (11) (2015) 4901~4911
www.springerlink.com/content/1738-494x(Print)/1976-3824(Online)
DOI 10.1007/s12206-015-1038-5

Adaptive fault detection and isolation for a class of robot manipulators with time-varying perturbation †

Amaneh Salmani Rezazadeh[1], Hamid Reza Koofigar[2,*] and Saeed Hosseinnia[1]

[1]*Department of Electrical Engineering, Najafabad Branch, Islamic Azad University, Najafabad, Iran*
[2]*Department of Electrical Engineering, University of Isfahan, Isfahan, Iran*

(Manuscript Received December 19, 2014; Revised June 4, 2015; Accepted July 2, 2015)

Abstract

This paper presents an adaptive-based fault detection and isolation scheme for a general class of robot manipulators, with characterizing the isolability conditions. The proposed algorithm consists of a nonlinear adaptive fault detection estimator and a bank of fault isolation estimators to determine the types of faults, which may be incipient or abrupt, while the fault parameter function may be time-varying. To demonstrate its effectiveness, the method is applied to a two-link robot manipulator and the simulation results are presented and discussed.

Keywords: Estimation; Fault detection; Robot manipulators; Time-varying parameters

1. Introduction

Robotic systems are extensively used in applications requiring high accuracy, reliability and safety. Industrial manufacturing, demining, hazardous waste cleanup, medical surgeries and outer space exploration are examples of various applications of such systems. With increasing the degrees of freedom and the number of components of robot manipulators, accurate monitoring of system malfunctioning has become more critical. In particular, the various faults that put the robot and the working environment at risk should be suitably detected and isolated.

In general, the procedure for dealing with faults may in-clude (i) detecting the occurrences of faults (fault detection), (ii) indicating faulty components (fault isolation), (iii) identifying features of faults (fault identification), and (iv) accommodating faults by dedicated control algorithms (fault tolerant control). In recent decades, fault detection and isolation (FDI) schemes have been investigated by many authors [1-3], and successfully applied to various safety systems such as nuclear plants [4], satellite systems [5], rolling element bearing [6, 7], hydraulic actuators [8, 9] and robotic systems [10, 11]. Such a problem is particularly challenging in a robot manipulator, as a Multi-input multi-output (MIMO) system, subjected to uncertainties, drastic nonlinearities and external disturbances. Concerning detecting and isolating faults in MIMO systems, there are commonly used techniques in the literature, such as state and parameter estimation [12-18], parity equations [19], neural networks [20-22], and multiple-model approaches [23-27]. In developing the FDI schemes, all of the state variables may be available for measurement [21, 23]. Such assumptions can be relaxed by designing some nonlinear observers, such as second-order sliding modes [15], in which the sensor fault signal is time invariant. The time-variance nature of the faults has been taken into account in some more recent schemes [22]. Of course, the robustness properties against model uncertainties and disturbances should be also ensured by the FDI algorithms [20, 22].

In this paper, we focus on the FDI problem for robotic manipulators with n-degrees-of-freedom, based on adaptive estimators. The fault is taken as a nonlinear function of both measurable and immeasurable states. Removing some of the previous restrictions, the main advantages of the proposed scheme are (i) using the soft sensor idea, the restriction of immeasurable states is overcome, (ii) distinguishing incipient faults and abrupt ones is possible, (iii) the fault parameter function may be time-varying, and (iv) the robustness property against unstructured uncertainties and external disturbances is ensured. Attaining such specifications, by using the proposed FDI scheme, is described more precisely via some remarks herein.

This paper is organized as follows. The mathematical model description of robot manipulators and the required assumptions are given in Sec. 2. The FDI architecture, the isolability conditions and the relevant proofs are derived in Sec. 3. An

*Corresponding author. Tel.: +98 31 37934081, Fax.: +98 31 37933071
E-mail address: koofigar@eng.ui.ac.ir
† Recommended by Associate Editor Kyoungchul Kong

illustrative example is given in Sec. 4 to demonstrate the effectiveness of the proposed method. Finally, the concluding remarks are presented in Sec. 5.

2. Mathematical model

The dynamic model of an n-degree-of-freedom rigid robot in the continuous time is given by

$$M(q(t))\ddot{q}(t) + n(q(t),\dot{q}(t)) = \tau(t) + \delta'(q,\dot{q},\tau,t), \tag{1}$$

where $q \in \Re^n$ denotes the joint position vector, $\tau \in \Re^n$ is the joint torque vector, $M(q) \in \Re^{n*n}$ represents the positive definite inertia matrix. The coriolis/centrifugal and frictional terms are collected in $n(q,\dot{q}) \in \Re^n$, and $\delta'(q,\dot{q},\tau,t) \in \Re^n$ includes the model uncertainties, low velocity friction, links flexibility and external disturbances.

Choosing a state vector as

$$\mathcal{q} = \begin{bmatrix} \mathcal{q}_1 \\ \mathcal{q}_2 \end{bmatrix} = \begin{bmatrix} q \\ \dot{q} \end{bmatrix}, \tag{2}$$

the state space equations of the robot manipulator can be written as

$$\begin{aligned} \dot{\mathcal{q}}(t) &= A\mathcal{q}(t) + h(\mathcal{q}(t)) + B(\mathcal{q}(t))\tau(t) \\ &\quad + \delta(\mathcal{q}(t),\tau(t),t) \\ y'(t) &= C'\mathcal{q}(t), \end{aligned} \tag{3}$$

where $A = \begin{bmatrix} O_n & I_n \\ O_n & O_n \end{bmatrix}, B = \begin{bmatrix} O_n \\ M^{-1}(\mathcal{q}(t)) \end{bmatrix}, C' = [O_n \quad I_n]$ and

$$h(\mathcal{q}(t)) = \begin{bmatrix} 0_n \\ -M^{-1}(q(t))n(q(t),\dot{q}(t)) \end{bmatrix}, \delta(\mathcal{q}(t),\tau(t),t) = \begin{bmatrix} 0_n \\ M^{-1}(q(t))\delta'(t,q(t),\dot{q}(t),\tau(t)) \end{bmatrix},$$

in which O_n denotes the $(n*n)$ null matrix, 0_n is the $(n*1)$ null vector, and I_n stands for the $(n*n)$ identity matrix.

Remark 1. Many FDI algorithms refer to the case that all the state variables are measurable [28]. In practice, only the velocitimeters are commonly used to measure $\mathcal{q}_2$. To tackle this limitation, a soft sensor is used here to generate $\mathcal{q}_1$ from $\mathcal{q}_2$ to be adapted in FDI estimators. The structure of this soft sensor is given by

$$\mathcal{q}_1 = \int_0^t y(t')dt' = \int_0^t \mathcal{q}_2(t')dt' = \int_0^t \dot{\mathcal{q}}_1(t')dt' + \mathcal{q}_1(0),$$

where the initial condition $\mathcal{q}_1(0)$ is known.

The mathematical model in the presence of the faults can be represented by

$$\begin{aligned} \dot{\mathcal{q}}(t) &= A\mathcal{q}(t) + h(\mathcal{q}(t)) + B(\mathcal{q}(t))\tau(t) \\ &\quad + \delta(\mathcal{q}(t),\tau(t),t) + \beta_{\mathcal{q}}(t - T_{\mathcal{q}})\psi((\mathcal{q}(t),\tau(t)) \\ y(t) &= C\mathcal{q}(t), \end{aligned} \tag{4}$$

where C is a constant matrix as $C = \begin{bmatrix} I_n & O_n \\ O_n & I_n \end{bmatrix}$. In Eq. (4), the changes in the robot manipulator dynamics due to actuator faults are characterized by $\beta_{\mathcal{q}}(t - T_{\mathcal{q}})\psi((\mathcal{q}(t),\tau(t))$, where $\beta_{\mathcal{q}}(t - T_{\mathcal{q}})$ denotes the time profile of an actuator fault, occurs at some unknown time $T_{\mathcal{q}}$, and $\psi((\mathcal{q}(t),\tau(t))$ represents the nonlinear fault function.

The fault time profile, $\beta(.)$ is adopted as a diagonal matrix of the form

$$\beta_i(t - T_{\mathcal{q}}) = \begin{cases} 0 & if \ t < T_{\mathcal{q}} \\ 1 - e^{-\alpha_i(t - T_{\mathcal{q}})} & if \ t \geq T_{\mathcal{q}} \end{cases}, \quad i = 1,\ldots,2n \tag{5}$$

where the scalar $\alpha_i > 0$ denotes the unknown fault evaluation rate.

Remark 2. Unlike some previous works in which the fault is only a function of input and output signals [29], such function may be dependent on all the state variables here. Moreover, the general form Eq. (5) facilitates taking both incipient and abrupt faults into account, respectively, by small values for α, and large ones, by which the time profile behaves like a step function.

As a preliminary step to design procedure, assume that there exist N types of possible faults in the fault set $\mathcal{F}$, i.e., the unknown fault function $\psi((\mathcal{q}(t),\tau(t))$ in Eq. (4) belongs to a finite set of fault types as

$$\mathcal{F} \triangleq \{\psi^1((\mathcal{q}(t),\tau(t))),\ldots,\psi^N((\mathcal{q}(t),\tau(t))\}, \tag{6}$$

where each fault type $\psi^p((\mathcal{q}(t),\tau(t))$ for $p = 1,\ldots,N$, is of the form

$$\psi^p(\mathcal{q}(t),\tau(t)) \triangleq \left[\left(\theta_1^p(t)\right)^T g_1^p(\mathcal{q}(t),\tau(t)),\ldots,\left(\theta_{2n}^p(t)\right)^T g_{2n}^p(\mathcal{q}(t),\tau(t))\right]^T \tag{7}$$

in which for $i = 1,\ldots,2n$, $\theta_i^p(t)$ is a time varying parameter vector and g_i^p is a known regressor with appropriate dimension.

Remark 3. Although the fault parameter is commonly assumed to be constant [28], it can be time-varying here.

The following assumptions are made for the system.

Assumption 1. The system states $\mathcal{q}_1$ and $\mathcal{q}_2$ remain bounded before and after the occurrence of any faults.

Assumption 2. There exists a bounded function, $\bar{\delta}$, such that the unstructured modeling uncertainty satisfies the inequality

$$|\delta(q(t),\tau(t),t)| \le \bar{\delta}(q(t),\tau(t),t). \tag{8}$$

Assumption 3. The unknown fault evaluation rate in Eq. (5) satisfies $\alpha_i > \bar{\alpha}$ where $\bar{\alpha}$ is a known lower bound and for simplifying the manipulation, take $\alpha_i = \alpha$, $i = 1, \ldots\ldots, 2n$. The rate of change of $\theta_i^p(t)$ in (7), $p = 1, \ldots, N$, is bounded as $|\dot{\theta}_i^p(t)| \le \gamma_p$ for all $t \ge 0$. In practice, the rate bound can be assigned by the designer, using some *a priori* knowledge of the fault developing dynamics.

3. Fault detection and isolation architecture

The structure of the FDI system is established here based on a bank of $N+1$ estimators, including a nonlinear adaptive estimator used to detect the occurrence of any faults, and remaining N estimators to determine the type of faults.

3.1 Fault detection scheme

Based on the robot manipulator dynamics Eq. (4), the architecture of Fault detection estimator (FDE) is chosen as

$$\begin{aligned}\dot{\hat{q}} &= A\hat{q} + h(q(t)) + B(q(t))\tau(t) + L(y-\hat{y})\\ \hat{y} &= C\hat{q},\end{aligned} \tag{9}$$

where $\hat{q}$ and $\hat{y}$ denote the estimated state and output vectors, respectively, and $L \in \Re^{2n*2n}$ is a gain matrix, chosen such that $\bar{A} \triangleq (A - LC)$ is Hurwitz. Defining $\tilde{q} \triangleq q - \hat{q}$ as the state estimation error, for $t < T_q$ one obtains

$$\dot{\tilde{q}}(t) = \bar{A}\tilde{q}(t) + \delta(q(t),\tau(t),t). \tag{10}$$

The j-th output estimation error $\tilde{y}_j(t) \triangleq y_j(t) - \hat{y}_j(t)$, $j = 1, \ldots.., 2n$, is determined by

$$\tilde{y}_j(t) = C_j\tilde{q}(t), \tag{11}$$

where C_j is the j-th row vector of matrix C. Using Eqs. (10) and (11), it can be bounded as

$$\begin{aligned}|\tilde{y}_j(t)| \le \textstyle\int_0^t \left[k_j e^{-\lambda_j(t-t')}|\delta(q(t'),\tau(t'),t')|\right]dt'\\ +k_j e^{-\lambda_j t}|\tilde{q}(0)|,\end{aligned} \tag{12}$$

in which k_j and λ_j are two positive constants, chosen such that $|C_j e^{\bar{A}t}| \le k_j e^{\lambda_j t}$ (since $\bar{A}$ is Hurwitz, such two constants always exist [30]).Taking into account the inequality Eq. (8) in Eq. (12) yields

$$\begin{aligned}|\tilde{y}_j(t)| \le \textstyle\int_0^t \left[k_j e^{-\lambda_j(t-t')}\left(\bar{\delta}(q(t),\tau(t'),t')\right)\right]dt'\\ +k_j e^{-\lambda_j t}|\tilde{q}(0)|.\end{aligned} \tag{13}$$

By Eq. (13), a fault is detected at $t = T_d$, whenever at least one component of the modulus of the output estimation error $\tilde{y}_j(t)$, exceeds its corresponding threshold $\bar{y}_j(t)$, specified by

$$\begin{aligned}\bar{y}_j(t) \triangleq \textstyle\int_0^t \left[k_j e^{-\lambda_j(t-t')}\left(\bar{\delta}(q(t'),\tau(t'),t)\right)\right]dt'\\ +k_j e^{-\lambda_j t}|\tilde{q}(0)|,\end{aligned} \tag{14}$$

and

$$T_d \triangleq inf \cup_{j=1}^{n} \{t \ge 0: |\tilde{y}_j(t)| > \bar{y}_j(t)\}, \tag{15}$$

in which inf stands for the infimum or the greatest lower bound. In this method, fault is detected immediately at $t = T_d$, whenever at least one component of the modulus of the output estimation error $\tilde{y}_j(t)$, exceeds its corresponding threshold $\bar{y}_j(t)$. However, in a second-order sliding mode algorithm [15], as a nonlinear observer, the residual is generated by evaluating the inverse dynamic model, which may be useful for identifying slow fault signals but produces some delays in the FDI procedure.

When a fault is detected at some time T_d, the Fault isolation estimators (FIEs), designed based on the functional structure of the actuator faults defined by Eqs. (6) and (7), are activated. The following N FIEs correspond to actuator fault p, $p = 1, \ldots.., N$.

$$\begin{aligned}\dot{\hat{q}}^p &= A\hat{q}^p + h(q(t)) + B(q(t))\tau(t)\\ &\quad +L^p(y(t) - \hat{y}^p(t)) + \Sigma^p(t)\dot{\hat{\theta}}^p(t)\\ &\quad +\hat{\psi}^p\left(\left(q(t),\tau(t),\hat{\theta}^p(t)\right)\right),\ \hat{q}^p(T_d) = 0\\ \dot{\Sigma}^p(t) &= \bar{A}^p\Sigma^p(t) + G^p(q(t),\tau(t)),\ \ \Sigma^p(T_d) = 0\\ \hat{\psi}^p &=\\ &[(\hat{\theta}_1^p)^T g_1^p(q(t),\tau(t)), \ldots.., (\hat{\theta}_{2n}^p)^T g_{2n}^p(q(t),\tau(t))]^T\\ \hat{y}^p &= C\hat{q}^p(t),\end{aligned} \tag{16}$$

where $\hat{\theta}_i^p$, $i = 1, \ldots.., 2n$ is the estimate of the fault parameter vector in the i-th state equation of the p-th isolation estimator and $L^p \in \Re^{2n*2n}$, is a design gain matrix chosen such that $\bar{A}^p \triangleq (A - L^pC)$ is Hurwitz. As the fault approximation model $\hat{\psi}^p$ is linear in the adjustable weights $\hat{\psi}^p$, the fault gradient matrix

$$\begin{aligned}G^p &= \frac{\partial\hat{\psi}^p\left(y(t),\tau(t),\hat{\theta}^p(t)\right)}{\partial\hat{\theta}^p(t)}\\ &= \mathrm{diag}[\left(g_1^p(y(t),\tau(t))^T, \ldots, g_{2n}^p(y(t),\tau(t))^T\right],\end{aligned}$$

is not dependent on $\hat{\theta}^p(t)$. Hence, it is sufficient to choose an adaptation mechanism for adjusting $\hat{\theta}^p$.

To ensure the robustness properties, a projection algorithm may be adopted as [30]

$$\dot{\hat{\theta}}^p(t) = \mathrm{proj}_{\Theta^p}\{\Gamma\Sigma^{p^T}C^T\tilde{y}^p\}, \tag{17}$$

where $\tilde{y}^p(t) \triangleq y(t) - \hat{y}^p(t)$ denotes the output estimation error of the p-th estimator, and $\Gamma > 0$ is a symmetric positive definite adaptation gain matrix.

While the fault function may be adopted as a function of state variables with time invariant intensity [28], it is taken here as a nonlinear function of state variable and torque signal with time variant intensity.

3.2 Adaptive threshold for fault isolation

One of the set of functions that plays a major role in fault isolation scheme is threshold functions set, represented here by $\mu_j(t)$. The following theorem presents a bounding function for the output estimation error of the p-th isolation estimator in the case that a fault occurs.

Theorem 1. If the actuator fault p occurs at time $t = T_q$ and is detected at $t = T_d$, then for all $t \geq T_d$, the j-th component of the output estimation error of the p-th isolation estimator satisfies the inequality

$$\begin{aligned}
\left|\tilde{y}_j^p(t)\right| \leq & \int_{T_d}^{t} k_j^p e^{-\lambda_j^p(t-t')}\,\bar{\delta}(q(t'),\tau(t'),t')dt' \\
&+\int_{T_d}^{t} k_j^p e^{-\lambda_j^p(t-t')}\,\|\Sigma^p(t')\|\left|\frac{d}{dt'}\left[e^{-\alpha(t'-T_q)}\hat{\theta}^p(t')\right]\right|dt' \\
&+\int_{T_d}^{t} k_j^p e^{-\lambda_j^p(t-t')}\dot{\hat{\theta}}^p(t)\|\Sigma^p(t')\|\,dt' \\
&+\int_{T_d}^{t} k_j^p e^{-\lambda_j^p(t-t')}\|\Sigma^p(t')\| \\
&\qquad\times\frac{d}{dt'}\left|\left(1-e^{-\alpha(t'-T_q)}\right)\tilde{\theta}^p(t')\right|dt' \\
&+\left|e^{-\alpha(t-T_q)}\right|\|\Sigma^p(t)\|\left|\hat{\theta}^p(t)\right| \\
&+\left|(1-e^{-\alpha(t-T_q)})\right|\|\Sigma^p(t)\|\left|\tilde{\theta}^p(t)\right| \\
&+k_j^p e^{-\lambda_j^p(t-T_d)}|\bar{q}(T_d)|, \qquad (18)
\end{aligned}$$

where $\tilde{\theta}^p(t) \triangleq \theta^p(t) - \hat{\theta}^p(t)$ is the parameter estimation error.

Proof. By Eq. (4), the system dynamic for $t > T_q$ is given by

$$\begin{aligned}
\dot{q}(t) &= Aq(t) + h\big(q(t)\big) + B\big(q(t)\big)\tau(t) \\
&\quad +\delta(q(t),\tau(t),t) + (1-e^{-\alpha(t-T_q)})\psi(q(t),\tau(t)) \\
y(t) &= Cq(t). \qquad (19)
\end{aligned}$$

In the presence of actuator fault $p, p = 1, \ldots, N$, let the state estimation error of the p-th isolation estimator be $\tilde{q}^p(t) \triangleq q(t) - \hat{q}^p(t)$. Hence, using Eqs. (16) and (19) yields

$$\begin{aligned}
\dot{\tilde{q}}^p(t) &= \left\{Aq(t) + h\big(q(t)\big) + B\big(q(t)\big)\tau(t)\right. \\
&\quad \left.+\delta(q(t),\tau(t),t) + (1-e^{-\alpha(t-T_q)})\psi((q(t),\tau(t))\right\} \\
&\quad -\left\{A\hat{q}^p + h\big(q(t)\big) + B\big(q(t)\big)\tau(t)\right. \\
&\qquad +L^p\big(y(t)-\hat{y}^p(t)\big) + \Sigma^p(t)\dot{\hat{\theta}}^p(t) \\
&\qquad \left.+\hat{\psi}^p\left(q(t),\tau(t),\hat{\theta}^p(t)\right)\right\} \\
&= \bar{A}^p\tilde{q}(t) + \delta(q(t),\tau(t),t) \\
&\quad +\big(1-e^{-\alpha(t-T_q)}\big)\psi\big(q(t),\tau(t)\big) - \Sigma^p(t)\dot{\hat{\theta}}^p(t) \\
&\quad -\hat{\psi}^p\left(q(t),\tau(t),\hat{\theta}^p(t)\right). \qquad (20)
\end{aligned}$$

Substituting $\psi(q,\tau) = G^p\theta^p$ and $\hat{\psi}^p(q,\tau) = G^p\hat{\theta}^p$ and some manipulations, results in

$$\begin{aligned}
\dot{\tilde{q}}^p(t) &= \bar{A}^p\tilde{q}^p(t) + \delta(q(t),\tau(t),t) \\
&\quad +\big(1-e^{-\alpha(t-T_q)}\big)G^p\big(q(t),\tau(t)\big)\theta^p(t) \\
&\quad -\Sigma^p(t)\dot{\hat{\theta}}^p(t) - G^p\big(q(t),\tau(t)\big)\hat{\theta}^p(t). \qquad (21)
\end{aligned}$$

Replacing $\tilde{\theta}^p(t) \triangleq \theta^p(t) - \hat{\theta}^p(t)$, and $\dot{\Sigma}^p(t)$ from Eq. (16) gives

$$\begin{aligned}
\dot{\tilde{q}}^p(t) &= \bar{A}^p\tilde{q}^p(t) + \delta(q(t),\tau(t),t) \\
&\quad +\big(1-e^{-\alpha(t-T_q)}\big)\left(\dot{\Sigma}^p(t) - \bar{A}^p(t)\Sigma^p(t)\right)\tilde{\theta}^p(t) \\
&\quad -\Sigma^p(t)\dot{\hat{\theta}}^p(t) \\
&\quad -e^{-\alpha(t-T_q)}\left(\dot{\Sigma}^p(t) - \bar{A}^p(t)\Sigma^p(t)\right)\hat{\theta}^p(t). \qquad (22)
\end{aligned}$$

By letting

$$\begin{aligned}
\bar{q}^p(t) &= \tilde{q}^p(t) + e^{-\alpha(t-T_q)}\Sigma^p(t)\hat{\theta}^p(t) \\
&\quad -\big(1-e^{-\alpha(t-T_q)}\big)\Sigma^p(t)\tilde{\theta}^p(t), \qquad (23)
\end{aligned}$$

and using Eq. (22), one obtains

$$\begin{aligned}
\dot{\bar{q}}^p(t) &= \dot{\tilde{q}}^p(t) - \big(1-e^{-\alpha(t-T_q)}\big)\dot{\Sigma}^p(t)\tilde{\theta}^p(t) \\
&\quad -\frac{d}{dt}\left[\big(1-e^{-\alpha(t-T_q)}\big)\tilde{\theta}^p(t)\right]\Sigma^p(t) \\
&\quad +e^{-\alpha(t-T_q)}\dot{\Sigma}^p(t)\hat{\theta}^p(t) \\
&\quad +\frac{d}{dt}\left[e^{-\alpha(t-T_q)}\hat{\theta}^p(t)\right]\Sigma^p(t) \\
&= \bar{A}^p\bar{q}^p(t) + \delta(q(t),\tau(t),t) \\
&\quad -\frac{d}{dt}\left[\big(1-e^{-\alpha(t-T_q)}\big)\tilde{\theta}^p(t)\right]\Sigma^p(t) \\
&\quad +\frac{d}{dt}\left[e^{-\alpha(t-T_q)}\hat{\theta}^p(t)\right]\Sigma^p(t) - \Sigma^p(t)\dot{\hat{\theta}}^p(t). \qquad (24)
\end{aligned}$$

By defining $\tilde{y}_j^p(t) \triangleq y_j(t) - \hat{y}_j^p(t)$ and using Eqs. (19) and (16), the output estimation error satisfies

$$\begin{aligned}
\tilde{y}_j^p(t) &= C_j\tilde{q}^p(t) \\
&= C_j\left(\bar{q}^p(t) - e^{-\alpha(t-T_q)}\Sigma^p(t)\hat{\theta}^p(t)\right. \\
&\qquad\qquad \left. + (1-e^{-\alpha(t-T_q)})\,\Sigma^p(t)\tilde{\theta}^p(t)\right), \qquad (25)
\end{aligned}$$

or

$$\begin{aligned}
\left|\tilde{y}_j^p(t)\right| \leq & \int_{T_d}^{t} k_j^p e^{-\lambda_j^p(t-t')}\,\bar{\delta}\big(q(t'),\tau(t'),t'\big)dt' \\
&+\int_{T_d}^{t} k_j^p e^{-\lambda_j^p(t-t')}\,\|\Sigma^p(t')\|\left|\frac{d}{dt'}\left[e^{-\alpha(t'-T_q)}\hat{\theta}^p(t')\right]\right|dt' \\
&+\int_{T_d}^{t} k_j^p e^{-\lambda_j^p(t-t')}\left|\dot{\hat{\theta}}^p(t)\right|\|\Sigma^p(t')\|\,dt' \\
&+\int_{T_d}^{t} k_j^p e^{-\lambda_j^p(t-t')}\|\Sigma^p(t')\|
\end{aligned}$$

$$\times \frac{d}{dt'}\left|\left(1-e^{-\alpha(t'-T_q)}\right)\tilde{\theta}^p(t')\right|dt'$$
$$+\left|-e^{-\alpha(t-T_q)}\right|\|\Sigma^p(t)\|\left|\hat{\theta}^p(t)\right|$$
$$+\left|\left(1-e^{-\alpha(t-T_q)}\right)\right|\|\Sigma^p(t)\|\left|\tilde{\theta}^p(t)\right|$$
$$+k_j^p e^{-\lambda_j^p(t-T_d)}|\tilde{q}(T_d).|. \quad (26)$$

Taking the absolute value of both sides of Eq. (26), the consequent Eq. (18) is concluded and this completes the proof.

Remark 4. As the estimation $\hat{\theta}^p(t)$ belongs to the unknown compact parameter set Θ^p one concludes $\left|\theta(t)-\hat{\theta}^p(t)\right| \le \kappa^p(t)$, where $\kappa^p(t)$ is dependent on the geometric properties of Θ^p. Moreover, incorporating assumption 3 into Eq. (18), the threshold functions for fault isolation are chosen as

$$\left|\mu_j^p(t)\right| \le \int_{T_d}^{t} k_j^p e^{-\lambda_j^p(t-t')}\,\bar{\delta}\left(q(t'),\tau(t'),t'\right)dt'$$
$$+\int_{T_d}^{t} k_j^p e^{-\lambda_j^p(t-t')}\left\|\Sigma^p(t')\right\|\left[\bar{\alpha}\, e^{-\bar{\alpha}(t'-T_q)}\left|\hat{\theta}^p(t')\right| + e^{-\bar{\alpha}(t'-T_q)}\gamma_p\right]dt'$$
$$+\int_{T_d}^{t} k_j^p e^{-\lambda_j^p(t-t')}\gamma_p\left\|\Sigma^p(t')\right\|dt'$$
$$+\int_{T_d}^{t} k_j^p e^{-\lambda_j^p(t-t')}\left\|\Sigma^p(t')\right\|\left(1-e^{-\bar{\alpha}(t'-T_q)}\right)\dot{\kappa}^p(t')dt'$$
$$+\int_{T_d}^{t} k_j^p e^{-\lambda_j^p(t-t')}\left\|\Sigma^p(t')\right\|\left(\bar{\alpha}e^{-\bar{\alpha}(t'-T_q)}\right)\kappa^p(t')dt'$$
$$+e^{-\bar{\alpha}(t-T_q)}\|\Sigma^p(t)\|\left|\hat{\theta}^p(t)\right|$$
$$+\left(1-e^{-\bar{\alpha}(t-T_q)}\right)\|\Sigma^p(t)\|\kappa^p(t)$$
$$+k_j^p e^{-\lambda_j^p(t-T_d)}|\bar{q}(T_d),| \quad (27)$$

in which k_j^p and λ_j^p are two positive constants, chosen such that $\left|C_j e^{\bar{A}^p t}\right| \le k_j^p e^{\lambda_j^p t}$.

Theorem 2. In the presence of faults in Eq. (4), the robust nonlinear fault isolation scheme formed by Eq. (16) guarantees that $\tilde{q}^p(t)$ and $\tilde{y}^p(t)$ are uniformly bounded, and there exists a positive constant ω and two bounded functions $\bar{\rho}_1^p(t)$ and $\bar{\rho}_2^p(t)$ such that for all $t_f \ge T_d$, the output estimation error satisfies the inequality

$$\int_{T_d}^{t_f}|\tilde{y}^p(t)|^2\,dt \le \omega + \left[\int_{T_d}^{t_f}\left|\bar{\rho}_1^p(t)\right|^2dt + \int_{T_d}^{t_f}\left|\bar{\rho}_2^p(t)\right|^2dt\right]. \quad (28)$$

Proof. The boundedness property and the closed loop stability are presented in two separate parts.

(i) *Boundedness*. The equation of state estimation error Eq. (21) can be rewritten as

$$\dot{\tilde{q}}_e^p(t) = \bar{A}^p\tilde{q}_e^p(t) + \delta(q(t),\tau(t),t)$$
$$+\left(1-e^{-\alpha(t-T_q)}\right)\psi^p((q(t),\tau(t),\bar{\theta}^p(t))$$
$$-\hat{\psi}^p\left(q(t),\tau(t),\hat{\theta}^p(t)\right)+\epsilon^p(t), \quad (29)$$

where $\epsilon^p(t)$ is called the bounded network approximation error and the parameter $\bar{\theta}^p$ is the value of $\hat{\theta}^p(t)$ that minimizes the L_∞ norm between $\psi((q(t),\tau(t))$ and $\hat{\psi}^p\left(q(t),\tau(t),\hat{\theta}^p(t)\right)$.

Now define

$$\bar{q}_e^p(t) = \tilde{q}_e^p(t) + e^{-\alpha(t-T_q)}\Sigma^p(t)\hat{\theta}^p(t)$$
$$+\left(1-e^{-\alpha(t-T_q)}\right)\Sigma^p(t)\theta_e^p(t), \quad (30)$$

and use Eq. (16) together with Eq. (29) to obtain

$$\dot{\bar{q}}_e^p(t) = \bar{A}^p\bar{q}_e^p(t) + \delta(q(t),\tau(t),t)$$
$$+\frac{d}{dt}\left[e^{-\alpha(t-T_q)}\right]\hat{\theta}^p(t)\Sigma^p(t)$$
$$+\frac{d}{dt}\left[\left(1-e^{-\alpha(t-T_q)}\right)\right]\Sigma^p(t)\theta_e^p(t) + \epsilon^p(t), \quad (31)$$

where $\theta_e^p(t) \triangleq \hat{\theta}^p(t) - \bar{\theta}^p$. The solution of Eq. (31) can be written as

$$\bar{q}_e^p(t) = \rho_1^p(t) + \rho_2^p(t), \qquad \forall t \ge T_d \quad (32)$$

in which $\rho_1^p(t)$ and $\rho_2^p(t)$ are the solutions of

$$\dot{\rho}_1^p(t) = \bar{A}^p\rho_1^p(t) + \delta(q(t),\tau(t),t)$$
$$+\frac{d}{dt}\left[e^{-\alpha(t-T_q)}\right]\hat{\theta}^p(t)\Sigma^p(t)$$
$$+\frac{d}{dt}\left[\left(1-e^{-\alpha(t-T_q)}\right)\Sigma^p\right](t)\theta_e^p(t) + \epsilon^p(t) \quad , \ \rho_1^p(T_d) = 0$$
$$\dot{\rho}_2^p(t) = \bar{A}^p\rho_2^p(t), \quad (33)$$

which yields

$$\left|\rho_1^p(t)\right| \le \int_{T_d}^{t_f}\left\|e^{\bar{A}^p(t-t')}\right\|$$
$$\times\left\|\delta\left(q(t'),\tau(t'),t'\right) + \frac{d}{dt'}\left[e^{-\alpha(t'-T_q)}\right]\hat{\theta}^p(\tau)\Sigma^p(t')\right.$$
$$\left.+\frac{d}{dt'}\left[\left(1-e^{-\alpha(t'-T_q)}\right)\right]\Sigma^p(t')\theta_e^p(t') + \epsilon^p(t')\right\|dt' \quad (34)$$

Taking Eq. (16), which ensures the boundedness of $\Sigma^p(t)$, and using assumptions 2 and 3 satisfies that the right hand side of Eq. (34) is bounded. Consequently, from the boundedness of $\rho_1^p(t)$ by Eq. (34) and $\rho_2^p(t)$ by Eq. (33), one concludes that $\bar{q}^p(t) \in L_\infty$ i.e., the signal boundedness property is proved.

(ii) *Stability*. Take the Lyapunov function candidate

$$V = \frac{1}{2}(\theta_e^p)^T\Gamma^{-1}\theta_e^p + \int_t^\infty\left|C\rho_2^p(t')\right|^2dt'. \quad (35)$$

Differentiating Eq. (35) and applying the projection algorithm Eq. (17) gives

$$\dot{V} \le (\theta_e^p)^T\Sigma^{p^T}C^T\tilde{y}^p - \left|C\rho_2^p(t)\right|^2$$
$$= \tilde{y}^{p^T}C\Sigma^p\theta_e^p - \left|C\rho_2^p(t)\right|^2.$$

Using Eq. (16) and completing the squares yields

$$\begin{aligned}\dot{V} &\le \tilde{y}^{p^T} C[\rho_1^p(t) + \rho_2^p(t) - e^{-\alpha(t-T_{q})}\Sigma^p(t)\hat{\theta}^p(t) \\ &\qquad -\tilde{q}^p(t)] - \left|C\rho_2^p(t)\right|^2 \\ &\le -|\tilde{y}^p|^2 + \tilde{y}^{p^T} C[\rho_1^p(t) + \rho_2^p(t) \\ &\qquad -e^{-\alpha(t-T_{q})}\Sigma^p(t)\hat{\theta}^p(t)] - \left|C\rho_2^p(t)\right|^2 \\ &\le -\frac{|\tilde{y}^p|^2}{4} \\ &\quad + \left[\left|C\rho_1^p(t)\right|^2 + \left|Ce^{-\alpha(t-T_{q})}\Sigma^p(t)\hat{\theta}^p(t)\right|^2\right]. \end{aligned} \tag{36}$$

Letting $\bar{\rho}_1^p(t) \triangleq 2\left(\left|C\rho_1^p(t)\right|^2\right)^{1/2}$ and $\bar{\rho}_2^p(t) \triangleq 2\left(\left|Ce^{-\alpha(t-T_{q})}\Sigma^p(t)\hat{\theta}^p(t)\right|^2\right)^{1/2}$ and integrating Eq. (36) from $t = T_d$ to $t = t_f$, one can obtain

$$\int_{T_d}^{t_f} |\tilde{y}^p(t)|^2\, dt \le \omega + \left[\int_{T_d}^{t_f} \left|\bar{\rho}_1^p(t)\right|^2 dt + \int_{T_d}^{t_f} \left|\bar{\rho}_2^p(t)\right|^2 dt\right], \tag{37}$$

where $\omega \triangleq \sup_{t_f \ge T_d}\{4[V(T_d) - V(t_f)]\}$ (sup is the supremum or the least upper bound), which completes the proof.

3.3 Fault isolability condition

Define a fault mismatch function of the form

$$h_j^{pr}(t) \triangleq C_j\left[\left(1 - e^{-\alpha(t-T_{q})}\right)\Sigma^p\theta^p - \Sigma^r\hat{\theta}^r\right] \quad r, p = 1, \ldots, N, \quad r \ne p. \tag{38}$$

In fact, the fault mismatch function is a filtered version of the difference between the actual p-th fault function, represented by $\left(1 - e^{-\alpha(t-T_{q})}\right)\Sigma^p\theta^p$ and some estimated fault function $\Sigma^r\hat{\theta}^r$.

The goal of introducing the fault isolability conditions is to specify the class of faults that can be isolated, i.e., the proposed fault isolation algorithm makes a correct decision in a finite time.

Theorem 3. The incipient fault p is isolable by the fault isolation scheme described by Eq. (30), if for each $p = 1, \ldots, N$ $(p \ne r)$, there exist some time $t^r > T_d$ and some $j = 1, \ldots, 2N$, so that h_j^{pr} defined by Eq. (38) satisfies the inequality

$$\begin{aligned}&\left|\int_{T_d}^{t} k_j^r e^{-\lambda_j^r(t^r - t')} h_j^{pr}(t')dt'\right| > \\ &2\int_{T_d}^{t} k_j e^{-\lambda_j(t-\tau)}\, \bar{\delta}\left(q(t'), \tau(t'), t'\right)dt' \\ &+ \int_{T_d}^{t} k_j\, e^{-\lambda_j(t-t')}\left[\bar{\alpha}\, e^{-\bar{\alpha}(t'-T_{q})}\left|\hat{\theta}^r(t')\right| + e^{-\bar{\alpha}(t'-T_{q})}\gamma_r \right. \\ &\qquad \left. + \bar{\alpha}\, e^{-\bar{\alpha}(t'-T_{q})}\left|\hat{\theta}^p(t')\right| + e^{-\bar{\alpha}(t'-T_{q})}\gamma_p\right]dt' \\ &+ \int_{T_d}^{t} k_j e^{-\lambda_j(t-t')}\left[\|\Sigma^r(t')\|\gamma_r + \|\Sigma^p(t')\|\gamma_p\right]dt' \\ &+ \int_{T_d}^{t} k_j e^{-\lambda_j(t-t')}\|\Sigma^r(t')\|\left(1 - e^{-\bar{\alpha}(t'-T_{q})}\right)\dot{\kappa}^r(t')dt' \\ &+ \int_{T_d}^{t} k_j e^{-\lambda_j(t-t')}\|\Sigma^r(t')\|\left(\bar{\alpha}e^{-\bar{\alpha}(t'-T_{q})}\right)\kappa^r(t')dt' \\ &+ e^{-\bar{\alpha}(t-T_d)}\left\|C_j\Sigma^p(t)\right\|\left|\hat{\theta}^p(t)\right| \\ &+ \left(1 - e^{-\bar{\alpha}(t-T_{q})}\right)\left\|C_j\Sigma^r(t)\right\|\kappa^r(t) \\ &+ 2k_j e^{-\lambda_j(t-T_d)}|\bar{q}(T_d)|. \end{aligned} \tag{39}$$

Proof. Using Eqs. (4) and (16), the dynamic equation of the r-th isolation estimation error $\tilde{q}^r(t) \triangleq q(t) - \hat{q}^r(t)$, in the presence of the p-th fault for $t > T_d$, satisfies

$$\begin{aligned}\dot{\tilde{q}}^r(t) &= \bar{A}^r\tilde{q}^r(t) + \delta(q(t), \tau(t), t) \\ &\quad + \left(1 - e^{-\alpha(t-T_{q})}\right)\left(\dot{\Sigma}^r(t) - \bar{A}^r(t)\Sigma^r(t)\right)\tilde{\theta}^r(t) \\ &\qquad - \Sigma^r(t)\dot{\hat{\theta}}^r(t) \\ &\quad - e^{-\alpha(t-T_{q})}\left(\dot{\Sigma}^r(t) - \bar{A}^r(t)\Sigma^r(t)\right)\hat{\theta}^r(t). \end{aligned} \tag{40}$$

Taking Eq. (25) into account, and some simple manipulations, one can obtain

$$\begin{aligned}\dot{\bar{q}}^r(t) &= \bar{A}^r\bar{q}^r(t) + \delta(q(t), \tau(t), t) \\ &\quad - \frac{d}{dt}\left[\left(1 - e^{-\alpha(t-T_{q})}\right)\tilde{\theta}^r(t)\right]\Sigma^p(t) \\ &\quad + \frac{d}{dt}\left[e^{-\alpha(t-T_{q})}\hat{\theta}^r(t)\right]\Sigma^r(t) - \Sigma^r(t)\dot{\hat{\theta}}^r(t). \end{aligned} \tag{41}$$

Based on Eq. (41), the j-th component of output estimation error satisfies

$$\begin{aligned}\tilde{y}_j^r(t) &= C_j\tilde{q}^r(t) \\ &= C_j\left(\bar{q}^r(t) - e^{-\alpha(t-T_{q})}\Sigma^p(t)\hat{\theta}^p(t) \right. \\ &\qquad \left. + \left(1 - e^{-\alpha(t-T_{q})}\right)\Sigma^p(t)\tilde{\theta}^p(t)\right). \end{aligned} \tag{42}$$

Incorporating Eq. (38) into Eq. (42) yields $\tilde{y}_j^r(t) = C_j\bar{q}^r(t) + h_j^{pr}(t)$. Meanwhile, following the proof of theorem 1 gives

$$\begin{aligned}\left|\tilde{y}_j^r(t)\right| &> \left|h_j^{pr}(t)\right| - \int_{T_d}^{t} C_j e^{-\bar{A}(t-t')}\,\bar{\delta}\left(q(t'), \tau(t'), t'\right)dt' \\ &- \int_{T_d}^{t} C_j e^{-\bar{A}(t-t')}\,\|\Sigma^p(t')\|\left|\frac{d}{dt'}\left[e^{-\alpha(\tau-T_{q})}\hat{\theta}^p(t')\right]\right|dt' \\ &- \int_{T_d}^{t} C_j e^{-\bar{A}(t-t')}\left|\dot{\hat{\theta}}^p(t)\right|\,\|\Sigma^p(t')\|\,dt' \\ &- \int_{T_d}^{t} C_j e^{-\bar{A}(t-t')}\|\Sigma^r(t')\| \\ &\qquad \times \frac{d}{dt'}\left|\left(1 - e^{-\alpha(t'-T_{q})}\right)\tilde{\theta}^r(t')\right|dt' \\ &- \left|-e^{-\alpha(t-T_{q})}\right|\|\Sigma^r(t)\|\left|\hat{\theta}^r(t)\right| \\ &- \left|\left(1 - e^{-\alpha(t-T_{q})}\right)\right|\|\Sigma^r(t)\|\left|\tilde{\theta}^r(t)\right| \\ &- C_j e^{-\bar{A}(t-\tau)}|\bar{q}(T_d)|. \end{aligned} \tag{43}$$

Taking the adaptive threshold Eq. (27) into account, if condition Eq. (39) is satisfied at time $t = t^r$; thus one obtains $\left|\tilde{y}_j^r(t^r)\right| > \mu_j^r(t^r)$, which implies that the possibility of the

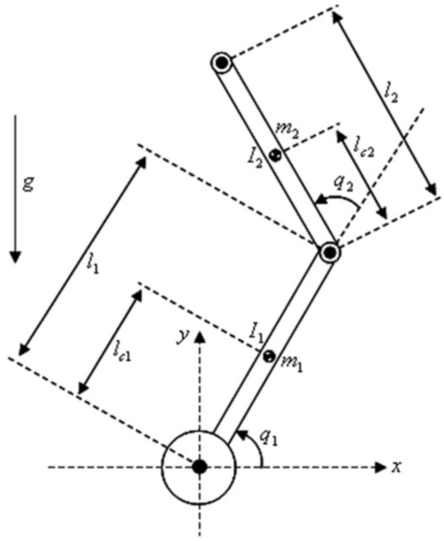

Fig. 1. Schematic of robot manipulator.

occurrence of fault p can be excluded at time $t = t^r$.

4. Simulation study

To illustrate the performance of the proposed FDI scheme, it is applied to a two-link planar robotic system. The dynamics of the manipulator, schematically shown in Fig. 1, is written as

$$\begin{bmatrix} s_1 + s_2 + 2s_3 cosq_2 & s_2 + s_3 cosq_2 \\ s_7 + s_8 cosq_2 & s_7 + s_9 \end{bmatrix} \begin{bmatrix} \dot{q}_1 \\ \dot{q}_2 \end{bmatrix} + \begin{bmatrix} -s_3 \dot{q}_2 sinq_2 & -s_3(\dot{q}_1 + \dot{q}_2) sinq_2 \\ s_8 \dot{q}_1 sinq_2 & 0 \end{bmatrix} \begin{bmatrix} \dot{q}_1 \\ \dot{q}_2 \end{bmatrix} + \begin{bmatrix} s_4 cosq_1 + \frac{g}{l_1} s_3 \cos(q_1 + q_2) \\ \frac{g}{l_1} s_8 cos(q_1 + q_2) \end{bmatrix} + \begin{bmatrix} s_5 \dot{q}_1 + s_6 sgn\dot{q}_1 \\ s_{10} \dot{q}_2 + s_{11} sgn\dot{q}_2 \end{bmatrix} = \begin{bmatrix} \tau_1 \\ \tau_2 \end{bmatrix}, \quad (44)$$

where s_i, $i = 1, \ldots, 11$, and the nominal values are introduced in Table 1 [31]. The system physical parameters are also given in Table 2. Moreover, $\begin{bmatrix} s_5 \dot{q}_1 + s_6 sgn\dot{q}_1 \\ s_{10} \dot{q}_2 + s_{11} sgn\dot{q}_2 \end{bmatrix}$ in Eq. (44) is considered as the system uncertainties, modeled by δ in dynamical Eq. (3).

First, a PID controller is developed for normal control of healthy system (without faults), as

$$\tau(t) = M(q(t)) \left[\ddot{q}_d(t) + k_d \dot{\tilde{q}}(t) + k_p \tilde{q} + k_I \int \tilde{q}(t) dt \right] + n(q(t), \dot{q}(t)),$$

where $q_d(t) \in \Re^n$ is desired joint position and defined tracking error $\tilde{q}(t) = q_d(t) - q(t)$, and k_p, k_d and k_I are PID gain matrices.

Table 1. Model parameters and their nominal values [31].

$s_1 = \left[(I_1 + m_1 l_{c_1}^2 + m_2 l_1^2) \, ^1/_{r_1^2} + J_1 \right] \, ^1/_{k_1}$	0.3339
$s_2 = (I_2 + m_2 l_{c_2}^2) \, ^1/_{r_1^2 k_1}$	0.0048
$s_3 = m_2 l_1 l_{c_2} \, ^1/_{r_2^2 k_1}$	0.0054
$s_4 = ((m_1 l_{c_1} + m_2 l_1) g) \, ^1/_{r_1^2 k_1}$	2.1450
$s_5 = b_1 \, ^1/_{k_1}$	2.8219
$s_6 = f_{c_1} \, ^1/_{r_1^2 k_1}$	1.5117
$s_7 = (I_2 + m_2 l_{c_2}^2) \, ^1/_{r_2^2 k_2}$	0.0240
$s_8 = m_2 l_1 l_{c_2} \, ^1/_{r_2^2 k_1}$	0.0280
$s_9 = J_2 \, ^1/_{r_2^2 k_2}$	0.00002
$s_{10} = b_2 \, ^1/_{k_2}$	1.2211
$s_{11} = f_{c_1} \, ^1/_{r_1^2 k_1}$	1.6282

Table 2. Description of the model parameters.

$I_1, (I_2)$	Moment of inertia of the 1st (2nd) line
$m_1, (m_2)$	Mass of the 1st (2nd) join
$l_1, (l_2)$	Length of the 1st (2nd) joint
$l_{c_1}, (l_{c_2})$	Distance from the joint to the C.G. of the 1st (2nd) link
$J_1, (J_2)$	Inertia of the motor's rotor of the 1st (2nd) joint
$r_1, (r_2)$	Gear ratio of the 1st (2nd) joint
$k_1, (k_2)$	Lumped constants of motors in the 1st (2nd) joint
$f_{c_1}, (f_{c_2})$	Coulomb friction coefficients of the 1st (2nd) joint
$b_1, (b_2)$	Combined viscous friction coefficients
g	Gravity acceleration

The desired trajectory in the joint space is chosen as [32]

$$q_{1_d} = -\frac{\pi}{2} + \frac{\pi}{4}\left(1 - e^{-2t^3}\right) + \frac{\pi}{9}\left(1 - e^{-2t^3}\right) sin(4t),$$
$$q_{2_d} = \frac{\pi}{3}\left(1 - e^{-2t^3}\right) + \frac{\pi}{6}\left(1 - e^{-2t^3}\right) sin(3t).$$

The gain matrices of PID controller are adopted as

$$k_p = \begin{bmatrix} 800 & 0 \\ 0 & 1500 \end{bmatrix}, \; k_d = \begin{bmatrix} 30 & 0 \\ 0 & 15 \end{bmatrix}, \; k_I = \begin{bmatrix} 1.411 & 0 \\ 0 & 0.3 \end{bmatrix}.$$

The multiplicative actuator faults take the form

$$\psi^i(q(t), \tau(t)) \triangleq \left(1 - e^{-\alpha(t - T_q)}\right) \times \left[\left(\theta_1^p(t)\right)^T g_1^p(q(t), \tau(t)), \ldots, \left(\theta_{2n}^p(t)\right)^T g_{2n}^p(q(t), \tau(t)) \right]^T$$

$p = 1, 2$, which results in two faults as fault 1 and fault 2 with the following properties.

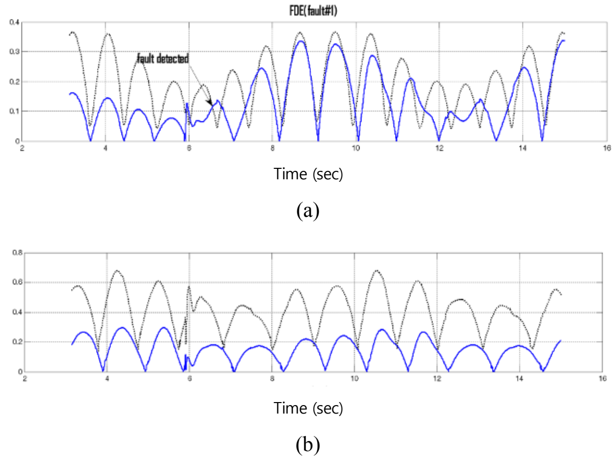

Fig. 2. (The case of fault 1) Fault detection residual (Solid line) and its threshold (Dotted line) associated with (a) y_3; (b) y_4.

Fault 1. For $i = 1$, $\theta^1 \in [-0.5\ \ 0.5]$ characterizes the magnitude of the fault. Note that the case $\theta^1 = 0$ represents the normal operation condition (no fault), while $\theta^1 = 0.5$ corresponds to the complete failure of the actuator. Therefore, the actuator fault can be described by

$$\psi^1\left(q(t), \tau(t)\right) = (1 - e^{-\alpha(t-T_q)})[0 \quad 0 \quad \theta_3^1 g_3^1 \quad 0]^T$$

where $g_3^1 = \left(0.5\frac{s_{10}}{s_8}\cos x_4\right)$ and $\theta_3^1 = 0.5(\cos(t^2))$.

Fault 2. For $i = 2$, $\theta^2 \in [-0.8\ \ 0.8]$ specifies the magnitude and the fault function is represented by

$$\psi^2\left(q(t), \tau(t)\right) = (1 - e^{-\alpha(t-T_q)})[0 \quad 0 \quad 0 \quad \theta_4^2 g_4^2]^T$$

where $g_4^2 = (1.4\,\frac{s_4}{s_8}\sin(x_3))$ and $\theta_4^2 = 0.8(\sin(t^2))$.

Based on the proposed FDI scheme, described in Sec. 3, a fault detection estimator and two fault isolation estimators are constructed. The initial condition of robot manipulator is assumed as $q(0) = 0$, the observer gain matrix L for fault detection as $L = diag(5,55,50,600)$, and the design constants $\lambda_3 = 35$, $\lambda_4 = 450$, $k_3 = 1$, $k_4 = 0.8$.

Throughout the simulations, to smoothen the function $sign(.)$ in Eq. (44), it is replaced by $tanh(r\,(.))$, where r is a sufficiently large constant.

The fault detection residual and its threshold associated with y_3, y_4, when fault 1 occurs at $T_q = 5.9$ sec with $\alpha = 0.5$, are depicted in Fig. 2. In fact, fault 1 is detected at approximately $T_d = 6.8$ sec. Then, two FIEs are activated to determine the occurring fault type. The matrix gain L^1 and L^2 for fault isolator Eq. (16) are chosen as

$$L^1 = \begin{bmatrix} 12 & 0 & 0 & 0 \\ 0 & 80 & 0 & 0 \\ 0 & 0 & 200 & 0 \\ 0 & 0 & 0 & 600 \end{bmatrix}, \; L^2 = \begin{bmatrix} 15 & 0 & 0 & 0 \\ 0 & 80 & 0 & 0 \\ 0 & 0 & 85 & 0 \\ 0 & 0 & 0 & 680 \end{bmatrix}.$$

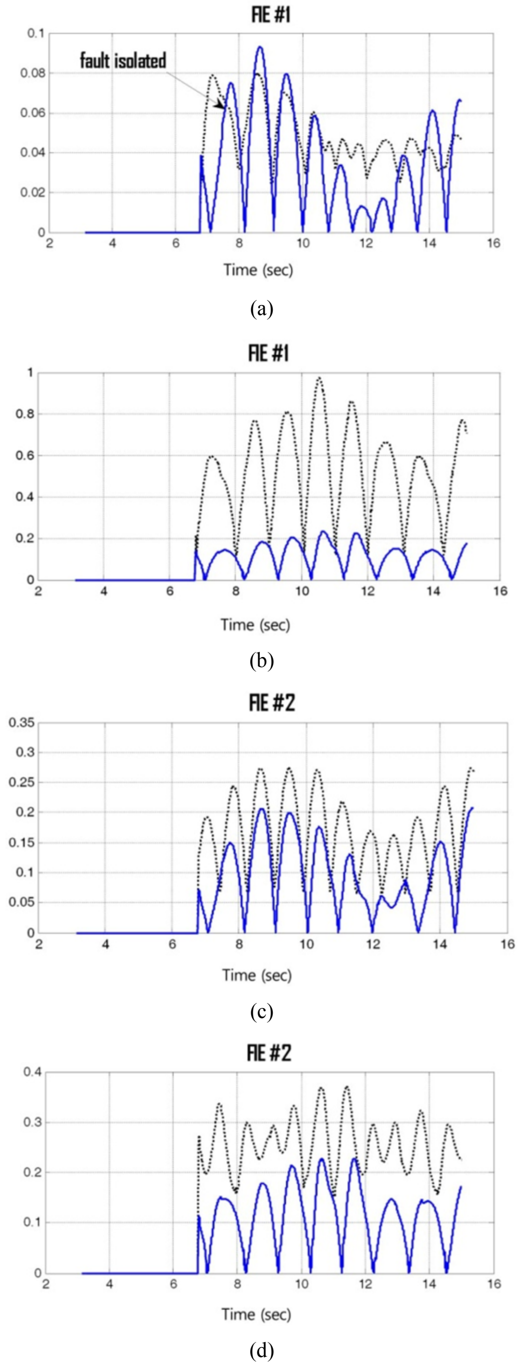

Fig. 3. Fault isolation residuals (Solid line) and their thresholds (Dotted line) associated with (a) y_3, generated by FIE 1; (b) y_4, generated by FIE 1; (c) y_3 generated by FIE 2; (d) y_4, generated by FIE 2.

Moreover, the design constants are $\lambda_3^1 = 75$, $\lambda_4^1 = 580$, $\lambda_3^2 = 55$, $\lambda_4^2 = 650$, $k_3^1 = 0.1$, $k_4^1 = 2.5$, $k_3^2 = 1$, $k_4^2 = 0.4$, and $\overline{\alpha} = 0.4$. The learning rates of the adaptive algorithm for fault parameter estimation in the FIEs are set to $\Gamma^1 = \mathrm{diag}(20, 20, 20, 20)$ and $\Gamma^2 = \mathrm{diag}(15, 15, 15, 15)$.

The fault isolation residuals and their corresponding thresholds, generated respectively by FIE 1 and FIE 2, are shown in Fig. 3. More precisely, Fig. 3(a) shows that the residual, asso-

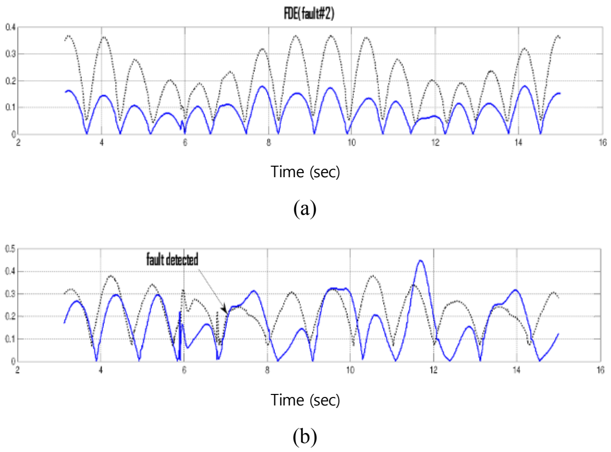

Fig. 4. (The case of fault 2) Fault detection residual (Solid line) and its threshold (Dotted line) associated with (a) y_3; (b) y_4.

ciated with y_3 and generated by FIE 1, exceeds its threshold, while in Figs. 3(b)-(d) all three residual components generated by the FIE 1 and FIE 2 always remain below their thresholds. Thus the occurrence of the actuator fault 1 is isolated at about $t_f = 7.6$ sec.

To show the ability of the method to isolate different faults with similar structures, the simulation results, when fault 2 occurs at $T_q = 5.9$ sec are shown in Figs. 4 and 5. Fig. 4 shows the results of FDE, in which fault 2 is detected almost immediately at $T_d = 6.3$ sec. Analogously, the fault isolation residuals and their corresponding thresholds generated, respectively, by FIE 1 and FIE 2, are shown in Fig. 5. Fig. 5(d) demonstrates that the residual, associated with y_4 and generated by FIE 2, exceeds its threshold and this is sufficient to exclude the possibility of occurrence of ψ^2 for fault isolation. On the other hand, Figs. 5(a)-(c) show that the other three residual components, generated by the FIE 1 and FIE 2, always remain below their thresholds, and consequently, the occurrence of fault 2 is isolated at about $t_f = 7.3$ sec.

However, considering fault 2 as the actuator fault, the presented FDI scheme in Ref. [28] is applied to the underlying robot. Fig. 6 demonstrates that such method can detect the fault type, but isolating the faulty state from other ones is not possible. Analyzing the simulation results confirms that the benefits of the proposed technique, claimed through the introduction, are achieved.

By increasing the number of links, the dimension of matrices in the model and the number of states would be increased. Compared with a two-link robot manipulator, except some more computations for larger matrices, no other changes would be made in the FDI procedure for an n-link robot manipulator.

5. Conclusions

Design and analysis of a unified adaptive FDI scheme is presented for robot manipulators with n degrees of freedom. Introducing the isolability conditions, the stability properties and adaptive learning capability were analyzed. A two-link robotic arm was adopted to illustrate the effectiveness of the proposed FDI method. As a future work, taking into account the both sensor fault and actuator fault is under investigation by the authors.

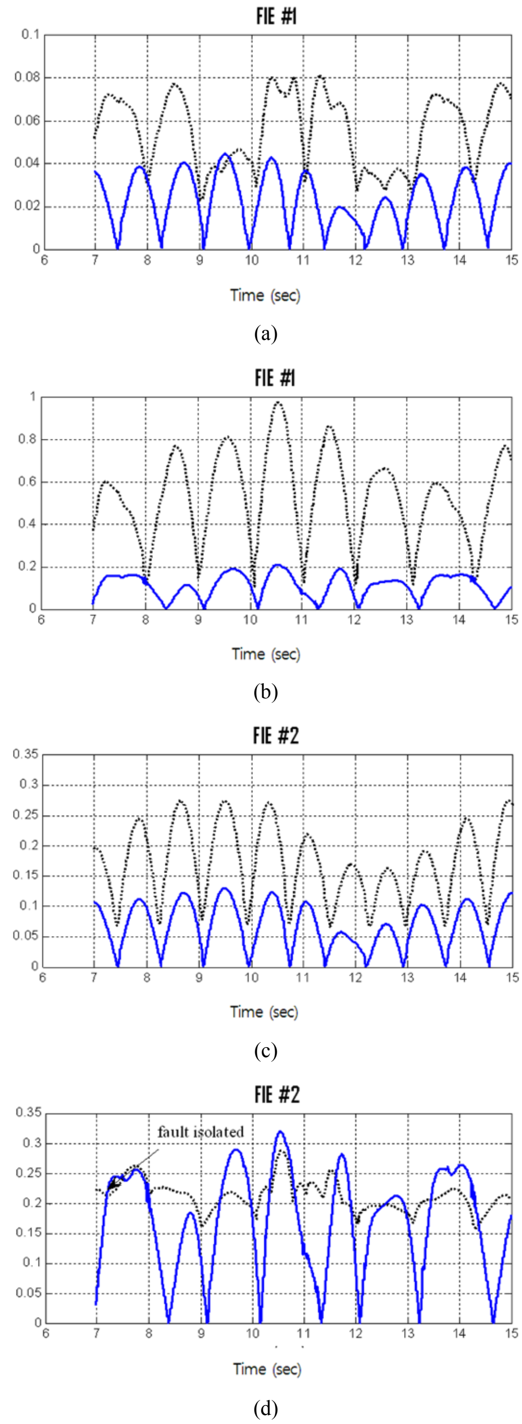

Fig. 5. Fault isolation residuals (Solid line) and their thresholds (Dotted line) with applying the proposed FDI scheme, associated with (a) y_3, generated by FIE 1; (b) y_4, generated by FIE 1; (c) y_3, generated by FIE 2; (d) y_4, generated by FIE #2.

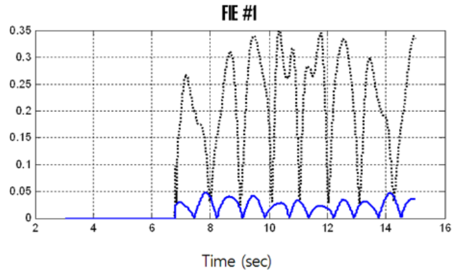

(a)

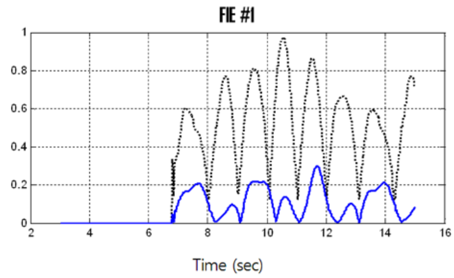

(b)

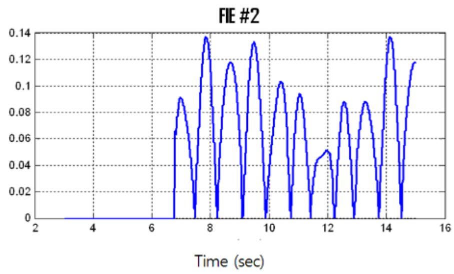

(c)

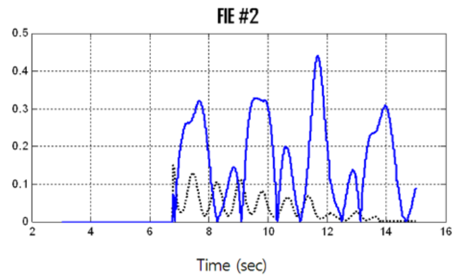

(d)

Fig. 6. Fault isolation residuals (Solid line) and their thresholds (Dotted line) with applying the FDI scheme in Ref. [28], associated with (a) y_3, generated by FIE #1; (b) y_4, generated by FIE #1; (c) y_3, generated by FIE #2; (d) y_4, generated by FIE #2.

References

[1] A. S. Willsky, A survey of design methods for failure detection in dynamic systems, *Automatica*, 12 (1976) 601-611.

[2] P. M. Frank, Fault diagnosis in dynamic systems using analytical and knowledge-based redundancy a survey and some new results, *Automatica*, 26 (1990) 459-474.

[3] R. Isermann, Process fault detection based on modeling and estimation methods a survey, *Automatica*, 20 (1984) 387-404.

[4] Q. Li and J. A. Bernard, Design and evaluation of an observer for nuclear reactor fault detection, *IEEE Trans. Nuclear Science*, 49 (2002) 1304-1308.

[5] D. S. Kim, S. M. Lee, J. H. Jung, T. H. Kim, S. Lee and J. S. Park, Reliability and availability analysis for an on board computer in a satellite system using standby redundancy and rejuvenation, *JMST*, 26 (7) (2012) 2059-2063.

[6] F. Cong, J. Chen and G. Dong, Spectral kurtosis based on AR model for fault diagnosis and condition monitoring of rolling bearing, *JMST,* 26 (2) (2012) 301-306.

[7] F. Zhang, Y. Liu, C. Chen, Y. F. Li and H. Z. Huang, Fault diagnosis of rotating machinery based on kernel density estimation and Kullback-Leibler divergence, *JMST,* 28 (2014) 4441-4454.

[8] A. Salmani, H. R. Koofigar and S. Hosseinnia, Robust leakage detection for electro hydraulic actuators using an adaptive nonlinear observer, *Int. J. Precision Engineering and Manufacturing,* 15 (3) (2014) 391-397.

[9] A. Y. Goharrizi and N. Sepehri, A wavelet-based approach for external leakage detection and isolation from internal leakage in valve-controlled hydraulic actuators, *IEEE Trans. Industrial Electronics*, 58 (2011) 4374-4384.

[10] M. L. Visinsky, J. R. Cavallaro and I. D. Walker, Robotic fault detection and fault tolerance: a survey, *Reliability Engineering and System Safety*, 46 (1994) 139-158.

[11] C. N. Cho, J. H. Kim, S. D. Lee and J. B. Song, Collision detection and reaction on 7 DOF service robot arm using residual observer, *JMST,* 26 (2012) 1197-1203.

[12] H. Liu and G. M. Coghill, A model-based approach to robot fault diagnosis, *Knowledge Based Systems*, 18 (2005) 225-233.

[13] F. Caccavale and L. Villani, *Fault Diagnosis and Fault Tolerance for Mechatronic Systems: Recent Advances*, Springer Verlag (2003) 71.

[14] H. Schneider and P. M. Frank, Observer-based supervision and fault detection in robots using nonlinear and fuzzy logic residual evaluation, *IEEE Trans. Control Systems Technology*, 4 (1996) 274-282.

[15] D. Brambilla, L. M. Capisani, A. Ferrara and P. Pisu, Fault detection for robot manipulators via second-order sliding modes, *IEEE Trans. Industrial Electronics*, 55 (2008) 3954-3963.

[16] W. E. Dixon, I. D. Walker, D. M. Dawson and J. P. Hartranft, Fault detection for robot manipulators with parametric uncertainty: a prediction-error based approach, *IEEE Trans Robotics and Automation*, 16 (2000) 689-699.

[17] M. L. McIntyre, W. E. Dixon, D. M. Dawson and I. D. Walker, Fault identification for robot manipulators, *IEEE Trans Robotics and Automation*, 2 (2005) 1028-1034.

[18] V. Verma, G. Gordon, R. Simmons and S. Thrun, Real-time fault diagnosis, *IEEE Trans Robotics and Automation*, 11 (2004) 56-66.

[19] V. F. Filaretov, M. K. Vukobratovic and A. N. Zhirabok, Parity relation approach to fault diagnosis in manipulation robots, *Mechatronics*, 13 (2003) 141-152.

[20] Q. Wu and M. Saif, Neural adaptive observer based fault detection and identification for satellite attitude control systems, *Proc. American Control Conference* (2005) 1054-1059.

[21] A. T. Vemuri, M. M. Polycarpou and S. A. Diakourtis, Neural network based fault detection in robotic manipulators, *IEEE Trans Robotics and Automation*, 144 (1998) 342-348.

[22] H. A. Talebi, K. Khorasani and S. Tafazoli, A recurrent neural-network-based sensor and actuator fault detection and isolation for nonlinear systems with application to the satellite's attitude control subsystem, *IEEE Trans Neural Networks*, 20 (2009) 45-60.

[23] M. Nyberg, Model-based diagnosis of an automotive engine using several types of fault models, *IEEE Trans Control Systems Technology*, 10 (2002) 679-689.

[24] Y. Zhang and X. R. Li, Detection and diagnosis of sensor and actuator failures using IMM estimator, *IEEE Trans. Aerospace and Electronic System*, 34 (1998) 1293-1313.

[25] N. Tudoroiu and K. Khorasani, Satellite fault diagnosis using a bank of interacting Kalman filters, *IEEE Trans. Aerospace and Electronic System*, 43 (2007) 1334-1350.

[26] S. Kim, J. Choi and Y. Kim, Fault detection and diagnosis of aircraft actuators using fuzzy-tuning IMM filter, *IEEE Trans. Aerospace and Electronic System*, 44 (2008) 940-952.

[27] J. Ru and X. R. Li, Variable-structure multiple-model approach to fault detection, identification, and estimation, *IEEE Trans Control Systems Technology*, 16 (2008) 1029-1038.

[28] S. N. Huang and K. K. Tan, Fault detection, isolation, and accommodation control in robotic systems, *IEEE Trans. Automation Science and Engineering*, 5 (2008) 480-489.

[29] X. Zhang, M. M. Polycarpou and T. Parisini, Design and analysis of a fault isolation scheme for a class of uncertain nonlinear systems, *Annual Reviews in Control*, 32 (2008) 107-121.

[30] P. A. Ioannou and J. Sun, *Robust Adaptive Control*, Prentice Hall, Englewood Cliffs, NJ (1996).

[31] H. A. P. Blom and Y. Shalom, The interacting multiple model algorithm for systems with Markovian switching coefficients, *IEEE Trans. Automatic Control*, 33 (1998) 780-783.

[32] T. Hsiao and M. C. Weng, A hierarchical multiple-model approach for detection and isolation of robotic actuator faults, *Robotics and Autonomous Systems*, 60 (2012) 154-166.

Amaneh Salmani Rezazadeh received the B.S. in Electrical Engineering and the M.S. in Control Engineering both from Islamic Azad University, Najafabad, Isfahan, Iran in 2009 and 2012, respectively. Her current research topics are fault detection and isolation, adaptive control and industrial automation.

Hamid Reza Koofigar received the M.S. degree in Control Engineering in 2005 and his Ph.D. in Electrical Engineering in 2009, both from Isfahan University of Technology, Iran. He joined the Department of Electrical Engineering, University of Isfahan in 2010, as Assistant Professor. His current research interests include robust control, adaptive nonlinear control, and robotics.

Saeed Hosseinnia received his M.S. from Oklahoma State University, Stillwater, USA in 1974 and Ph.D. from Isfahan University of Technology (IUT), Isfahan, Iran in 2000 both in Electrical Engineering. He is currently an Assistant Professor of Electrical Engineering at Islamic Azad University-Najafabad Branch, Najafabad, Iran. His research interests include system theory, nonlinear control and robust control.